A Theoretical and Numerical Approach for Selecting Miniaturized Antenna Topologies on Magneto-Dielectric Substrates

A. Pacini[1], A. Costanzo[1,2], D. Masotti[2]

[1]DEI – "Guglielmo Marconi"; II School of Architecture and Engineering, University of Bologna, Cesena Campus, Italy

[2]DEI – "Guglielmo Marconi"; School of Architecture and Engineering, University of Bologna, Bologna, Italy

An increasing interest is arising in developing miniaturized antennas in the microwave range. However, even when the adopted antennas dimensions are small compared to the wavelength, radiation performances have to be preserved in order to keep the system operating conditions. For this purpose, magneto-dielectric materials are currently exploited as promising substrates which allows to reduce antenna dimensions by exploiting both relative permittivity and permeability. In this paper we address generic antennas in resonant conditions and we develop a general theoretical approach, not based on simplified equivalent models, to establish topologies most suitable for exploiting high permeability and/or high permittivity substrates, for miniaturization purposes. A novel definition of the region pertaining to the antenna near-field and of the associated field strength is proposed. It is then showed that radiation efficiency and bandwidth can be preserved only by a selected combinations of antenna topologies and substrate characteristics. Indeed, by the proposed independent approach, we confirm that non-dispersive magneto-dielectric materials with relative permeability greater than unit, can be efficiently adopted only by antennas that are mainly represented by equivalent magnetic sources. Conversely, if equivalent electric sources are involved, the antenna performance are significantly degraded. The theoretical results are validated by full-wave numerical simulations of reference topologies.

Keywords: Authors should not add keywords, as these will be chosen during the submission process (see http://journals.cambridge.org/data/relatedlink/MRF_topics.pdf for the full list)

Corresponding author: A. Pacini; email: alex.pacini@ieee.org; phone: +39 3383692711

I INTRODUCTION

There are a variety of new application areas in which it is needed to achieve ultra-small wireless systems, such that they can be worn [1], and/or implanted under the tissues [2] (e.g. in the case of biomedical devices). To accomplish this, it is required that the antenna system provides extremely reduced dimensions while preserving the best radiation performance to minimize the power consumption. This is a challenging task since it is well known that for best antenna operation its dimensions need to be proportionally related to

the wavelength. In the *UHF* band, where the majority of these applications are developed, the latter is of the order of hundred millimetres. For this purpose, in the last few years, a significant research effort has been dedicated to the strategic use of design techniques and materials enabling the miniaturization of the components while maintaining the best possible performance. A highly exploited solution to build miniaturized and non-invasive antennas is the patch antenna mounted on dense dielectric substrate. The reduced effective wavelength λ_g is obtained at the expense of an increased patch-ground plane coupling, thus reducing the *field fringing effect*: in this way, the radiating properties of the antenna may be degraded and the patch behaves more as a microstrip resonator. Indeed a significant reduction of the radiation resistance is observed, which causes a decay in radiation efficiency. At the same time a too low antenna impedance is obtained, which is difficult to be matched. An emerging alternative to dense dielectrics is provided by the recent realization of materials characterized by relative magnetic permeability μ_r greater than unit [3–6]. They could overcome the above-mentioned limitations since, for a given relative permittivity and permeability ε_r and μ_r, they could simultaneously guarantee the required guided-wavelength reduction while controlling the medium impedance.
Previously, theoretical models were proposed [7] in order to choose the best substrate material according to a certain resonating antenna topology. The simplest approach was to use the *RLC* resonator equivalent circuit as representative of the behaviour of the antenna at resonance. If the antenna behaves as a *parallel* resonator an *Only Magnetic (OM)* is convenient, while as a *series* resonator an *Only Dielectric (OD)* is better suited. This model can be successfully adopted for simple topologies but can be inaccurate in more complex antenna layouts, such as Planar Inverted L-Antenna[7]. The qualitative explanation lays on inaccuracies when modelling a true three-dimensional structure with a one-dimensional lumped circuits representation. Moreover, the energy stored in the field can not be represented as the energy stored in an RLC circuit, given its complex structure [9], and the radiation resistance can vary (thus the RLC quality factor).
Another possible model is based on the transmission line theory [7]. This approach was used in a previous attempt in [8] to analytically provide a proof for the patch antenna. Again, given a generic antenna topology, its geometry and radiation properties are not accurately derivable from the transmission line parameters, as for example, the transmission line characteristic impedance.
A very interesting theoretical approach has been conjectured in [7]. It is based on the *antenna equivalent current sources* for establishing a set of design rules for antennas on magneto-dielectric substrates.
The aim of this work is to validate these rules. For this purpose, for the first time, we are able to theoretically demonstrate a general method for resonant antennas suitable for a generic source distribution in a volume, that is a generic resonant antenna layout. This is obtained by subsequently considering these sources surrounded by the empty space and by a non dispersive magneto-dielectric medium. We then theoretically develop the relations between the fields in the two different media. A straightforward application of the Love's principle of equivalence [10], allows us to compute the associated equivalent current sources, confirming by an independent and general way the surface current relation as in [7].
The main validation results were proposed in [14], but in this paper we develop a complete rigorous and detailed analytical solution to obtain the relation between the fields. Such procedure is based on the Wilcox series [15] and on the uniqueness theorem in spite of a

simple functions product, to represent the electromagnetic fields in the computation of the energy integrals. This allows us to provide a rigorous evaluation of the antenna radiation characteristics. In particular, we provide general analytical expressions for the radiated power, the energy stored, the quality factor, the losses and thus the radiation efficiency and the bandwidth. An extension of the theory to a more general hypothesis between the fields is provided.
An extensive validation procedure based on full-wave numerical simulations [11] is also provided.
We selected a patch antenna topology, which can be modelled by magnetic sources, to validate the proposed fields relations by using different substrate, namely the OM and the ES, and far-field predictions are included. Furthermore, we considered two printed loop antennas on OD and OM materials, which can be modelled by electric sources, and their bandwidth characteristics are compared with those belonging to the patch antennas on the same materials. It is noteworthy that the antennas geometries have been tuned in such a way that they provide the same resonance frequency. In practice this is equivalent to consider the dimensions related to the guided wavelength, accounting for the effective media constitutive parameters instead of the relative ones.

II THEORETICAL FORMULATION

Let us analyse the behaviour of resonant antennas, surrounded by different isotropic media, in terms of their equivalent current sources and volumes involved. Resonant antennas are chosen since they guarantee the best radiation efficiency, which is mandatory when only ultra-low power excitations are available. For the sake of simplicity, we neglect both dielectric and magnetic losses and assume that the materials are non-dispersive. The former assumption can be easily removed by the application of the perturbation theory [13]. The latter is verified by the material considered in [5], such as hexaferrites that must operate well below the Ferro-Magnetic Resonance (FMR), thus providing a fairly constant permeability all over the operative bandwidth.

A) Computation of the equivalent antenna current sources

First let us consider an antenna immersed in empty space (*ES*) satisfying the resonance conditions. The magnetic energy at resonance can be computed in a defined volume V_{n-f}, which includes the whole near-field generated by the antenna, thus the energy stored satisfies the following equality:

$$\int_{V_{n-f}} \mu_0 \left|\mathbf{H}(r,\theta,\phi)\right|^2 \, dV = \int_{V_{n-f}} \varepsilon_0 \left|\mathbf{E}(r,\theta,\phi)\right|^2 \, dV \tag{1}$$

It is noteworthy that the integration volume should be carefully selected to be large enough to include the entire near-field region, but limited to avoid divergence in (1) due to the far-field contribution. Its exact definition is dependent on the particular circumstances, theoretical or practical, but it is not an issue and is stated case by case in the following.
Let us now substitute the ES with an another isotropic medium: in this case we adopt an OM material with permeability $\mu_r\mu_0$ and permittivity ε_0. We can reasonably suppose that

the volume containing the OM material-antenna near-field ($V_{n-f}^{(\mu)}$) is reduced, with respect to the ES case, according to the rule relating the guided wavelength to the relative electromagnetic constants. Accordingly, we assume that the same energy balance computed by (1) can be obtained in the reduced volume:

$$V_{n-f}^{(\mu)} = \frac{V_{n-f}}{\sqrt{\mu_r^3}} \tag{2}$$

where it will be:

$$\int\limits_{V_{n-f}^{(\mu)}} \mu_0\mu_r \left|\mathbf{H}_\mu(r_\mu,\theta,\phi)\right|^2 \, dV^\mu = \int\limits_{V_{n-f}^{(\mu)}} \varepsilon_0 \left|\mathbf{E}_\mu(r_\mu,\theta,\phi)\right|^2 \, dV^\mu \tag{3}$$

Now, as an hypothesis, we can adopt the following relationship between the corresponding electric field in the ES ($\mathbf{E}$) and in the OM ($\mathbf{E}_\mu$):

$$\left|\mathbf{E}(r,\theta,\phi)\right| = \mu_r^{-\frac{1}{2}} \left|\mathbf{E}_\mu(r_\mu,\theta,\phi)\right| \tag{4}$$

where

$$r_\mu = r\mu_r^{-\frac{1}{2}} \tag{5}$$

These relationships rely on the condition of obtaining the same radiated power in the far-field with a reduced wavelength, due to the adopted substrate, for a patch antenna without losses (4). These results are also validated in the next section by the numerical simulation for two patch antennas. Notice μ_r should be thought as an effective value.
Let us now adopt the variable substitutions (2), for dV^μ, and (5) for r_μ, and the hypothesis (4) and (1) to compute equation (3) which becomes:

$$\int\limits_{V_{n-f}^{(\mu)}} \varepsilon_0 \left|\mathbf{E}_\mu(r_\mu,\theta,\phi)\right|^2 \, dV^\mu = \mu_r^{-\frac{1}{2}} \int\limits_{V_{n-f}} \mu_0 \left|\mathbf{H}(r,\theta,\phi)\right|^2 \, dV \tag{6}$$

The LHS (Left Hand Side) of (3) by substitutions can also be cast:

$$\int\limits_{V_{n-f}^{(\mu)}} \mu_0\mu_r \left|\mathbf{H}_\mu(r_\mu,\theta,\phi)\right|^2 \, dV^\mu = \mu_r^{-\frac{1}{2}} \int\limits_{V_{n-f}} \mu_0 \left|\mathbf{H}_\mu(r_\mu,\theta,\phi)\right|^2 \, dV \tag{7}$$

Thus we can write:

$$\int\limits_{V_{n-f}} \left|\mathbf{H}(r,\theta,\phi)\right|^2 \, dV = \int\limits_{V_{n-f}} \left|\mathbf{H}_\mu(r_\mu,\theta,\phi)\right|^2 \, dV \tag{8}$$

where $\mathbf{H}_\mu$ is the magnetic field in the OM case.
The magnetic fields relation satisfying (8) can be obtained by resorting to a modified Wilcox expansion [15]:

$$\left|\mathbf{H}_\mu(r_\mu,\theta,\phi)\right| = \left|\sum_{n=0}^{\infty} c_{n,\mu} \, \frac{\mathbf{B}_n(\theta,\phi)}{r_\mu^{n+1}}\right| \tag{9a}$$

$$\left|\mathbf{H}(r,\theta,\phi)\right| = \left|\sum_{n=0}^{\infty} c_n \, \frac{\mathbf{B}_n(\theta,\phi)}{r^{n+1}}\right| \tag{9b}$$

This representation is addressed as *modified* due to the presence of the $c_{n,\mu}$ and c_n terms, which are dependent only on the substrate material; it is noteworthy that the vector function $\mathbf{B}_n(\theta,\phi)$, representing the dependence on the elevation and azimuth variables, is the same for both expansions, i.e. when $n=0$ the two antennas share the same shape of the radiation functions.
Now it is possible to represent (8) using (9); its RHS (Right Hand Side), considering (5) and (9a), becomes:

$$\int\limits_{V_{n-f}} |\mathbf{H}_\mu(r_\mu,\theta,\phi)|^2 \; dV = \mu_r^{\frac{m+n+2}{2}} \int\limits_{V_{n-f}} \sum_{m=0}^{\infty}\sum_{n=0}^{\infty} c_{m,\mu}c_{n,\mu}^* \, \frac{\mathbf{B}_m(\theta,\phi)\cdot\mathbf{B}_n^*(\theta,\phi)}{r^{m+n+2}} \, dV \tag{10}$$

Similarly, by using (9b) in the LHS of (8), (8) becomes:

$$\int\limits_{V_{n-f}} \sum_{m=0}^{\infty}\sum_{n=0}^{\infty} \left(\frac{\mathbf{B}_m(\theta,\phi)\cdot\mathbf{B}_n^*(\theta,\phi)}{r^{m+n+2}}\right)\left(\frac{c_{m,\mu}c_{n,\mu}^*}{\mu_r^{-\frac{m+n+2}{2}}} - c_m c_n^*\right) \, dV = 0 \tag{11}$$

The LHS and RHS integrals in (1), and thus in (8), are singularly divergent due to the radiated power in the far-field [9]. But, since a difference is computed inside (11) and the far-field radiated powers were forced to be the same for both materials, the integral in (11) is not divergent any more. Mathematically, given the above consideration, the volume can be thought as going to infinite. This removes the ambiguity in its definition for this theoretical case, but for completeness and easiness of notation, in what follows is still specified as V_{n-f}.
Furthermore, since the Poynting vector is not divergent, it is also possible to swap the integral and sums [9] to get:

$$\sum_{m=0}^{\infty}\sum_{n=0}^{\infty}\left(\int\limits_{V_{n-f}} \frac{\mathbf{B}_m(\theta,\phi)\cdot\mathbf{B}_n^*(\theta,\phi)}{r^{m+n+2}} \, dV\right)\left(\frac{c_{m,\mu}c_{n,\mu}^*}{\mu_r^{-\frac{m+n+2}{2}}} - c_m c_n^*\right) = 0 \tag{12}$$

Considering the same boundary conditions, equation (12) has multiple solutions. There are different relations regarding the various c coefficients and thus the field within the OM. By using the *uniqueness theorem* the field has to be unique. Here we consider the solution by zeroing all the terms of the series:

$$c_{m,\mu}c_{n,\mu}^* = \mu_r^{-\frac{m+n+2}{2}} \; c_m c_n^* \tag{13}$$

By using (5) and (13) into (9a), the relationship between $\mathbf{H}_\mu$ and $\mathbf{H}$ becomes:

$$|\mathbf{H}_\mu(r_\mu,\theta,\phi)|^2 = |\mathbf{H}(r,\theta,\phi)|^2 \;\Rightarrow\; |\mathbf{H}_\mu(r_\mu,\theta,\phi)| = |\mathbf{H}(r,\theta,\phi)| \tag{14}$$

The solution for the OM material is validated by solving the homogeneous Helmholtz equation in the domain (r_μ):

$$\nabla_\mu^2 \, \mathbf{H}_\mu(r_\mu,\theta,\phi) = \mu\varepsilon_0 \, \frac{\partial^2}{\partial t^2} \, \mathbf{H}_\mu(r_\mu,\theta,\phi) \tag{15}$$

which by substituting (5) results in:

$$\nabla^2 \mathbf{H}(r,\theta,\phi) = \mu_0 \varepsilon_0 \frac{\partial^2}{\partial t^2} \mathbf{H}(r,\theta,\phi) \tag{16}$$

hence if $\mathbf{H}(r,\theta,\phi)$ is a valid solution to the homogeneous Maxwell equations, $\mathbf{H}_\mu(r_\mu,\theta,\phi)$ is also valid, in particular it is the same solution in the corresponding spatial domain.
Relation (14) will be numerically validated later.
It is known that the far-field has TEM properties, it is thus easy to express the relation in (4) and (14) as the components tangent to the contour sphere of the volume $(V_\infty - V_{n-f})$:

$$|\mathbf{E}_\tau| = \mu_r^{-\frac{1}{2}} \left|\mathbf{E}_\tau^{(\mu)}\right| \ , \ |\mathbf{H}_\tau| = \left|\mathbf{H}_\tau^{(\mu)}\right| \tag{17}$$

Notice that the relations (4) and (14) have been extended to be valid outside the V_{n-f}, since the term in the Wilcox expansion (9) with $n = 0$ is present even in the near-field and the near-field volume could be theoretically extended to $r \to \infty$, as also said in [9].
We can now make use of the Love's field equivalence principle [10] to get the corresponding electric and magnetic magnitude of surface equivalent currents $\mathbf{J}_S$, $\mathbf{J}_S^{(\mu)}$ and $\mathbf{M}_S$, $\mathbf{M}_S^{(\mu)}$:

$$\left|\mathbf{J}_S^{(\mu)}\right| = |\mathbf{J}_S| = |\hat{n} \times \mathbf{H}_\tau| \ , \ \left|\mathbf{M}_S^{(\mu)}\right| = \sqrt{\mu_r}\,|\mathbf{M}_S| = |\mathbf{E}_\tau \times \hat{n}| \tag{18}$$

where $\hat{n}$ is the versor normal to the surface.
From (18) is noteworthy that the equivalent electric sources are not affected by the introduction of a magnetic material, while the equivalent magnetic sources are increased by a factor $\sqrt{\mu_r}$, in the respective domain.
By means of the duality principle an OD material can be described following the same steps, thus providing results similar to (18), with the superscript (ε) indicating the vectors in the OD case:

$$\begin{gathered} |\mathbf{E}_\tau| = \left|\mathbf{E}_\tau^{(\varepsilon)}\right| \ , \ |\mathbf{H}_\tau| = \varepsilon_r^{-\frac{1}{2}} \left|\mathbf{H}_\tau^{(\varepsilon)}\right| \\ \left|\mathbf{J}_S^{(\varepsilon)}\right| = \sqrt{\varepsilon_r}\,|\mathbf{J}_S| = |\hat{n} \times \mathbf{H}_\tau| \ , \ \left|\mathbf{M}_S^{(\varepsilon)}\right| = |\mathbf{M}_S| = |\mathbf{E}_\tau \times \hat{n}| \end{gathered} \tag{19}$$

It is noteworthy that, differently from the OM case, the dual hypothesis on $\mathbf{H}$ in (19) does not provide a constant radiated power in the far-field for a patch antenna, but it is a purely mathematical assumption derived from the duality theorem.

B) Computation of the antenna radiation characteristics

The near-field properties provided by (4), (14) and (18) can also be adopted for the far-field vectors, thus we can evaluate the active radiated power, the energy stored and the losses of antennas exploiting an OM material and ES as substrates; it is then possible to obtain the relations for bandwidth and efficiency.
By referring to the Poynting vector dependence in the far field, the domain dependence can be removed. The absolute value of the Poynting vector for ES and OM in the domain r results as:

$$\begin{aligned} S_{J_S}^{(\mu)}(r,\theta,\phi) &= \mu_r^{-1}\, S_{J_S}(r,\theta,\phi) \\ S_{M_S}^{(\mu)}(r,\theta,\phi) &= S_{M_S}(r,\theta,\phi) \end{aligned} \tag{20}$$

According to the results described in the previous subsection, it is clear that the miniaturization by means of an OM material is not convenient in case of an antenna exploiting electrical equivalent currents $\mathbf{J}_S$. Conversely, for antennas exploiting magnetic equivalent currents $\mathbf{M}_S$, an OM substrate allows a suitable antenna dimensions reduction since it preserves the radiation performances without affecting the active radiated power density with respect to ES.
The power density (20) allows to straightforwardly calculate the radiated power (P):

$$P_{J_S}^{(\mu)} = \mu_r^{-1}\, P_{J_S}\ ,\ P_{M_S}^{(\mu)} = P_{M_S} \tag{21}$$

while using (4) for the stored energy (W) we can write:

$$W_E^{(\mu)} = \mu_r^{-\frac{1}{2}}\, W_E \quad \Rightarrow \quad W_{TOT}^{(\mu)} = \mu_r^{-\frac{1}{2}}\, W_{TOT} \tag{22}$$

Notice that (20), (21) and (22) are strictly dependent on the initial hypothesis (4).
It is now immediate to get the quality factor and thus approximately the bandwidth:

$$\begin{aligned} Q_{J_S}^{(\mu)} &= 2\pi f_r\, \frac{\mu_r^{-\frac{1}{2}}\, W_{TOT}}{P_{J_S}\, \mu_r^{-1}} = \mu_r^{\frac{1}{2}}\, Q_{J_S} \ \Rightarrow\ BW_{J_S}^{(\mu)} \sim \frac{BW_{J_S}}{\mu_r^{\frac{1}{2}}} \\ Q_{M_S}^{(\mu)} &= 2\pi f_r\, \frac{\mu_r^{-\frac{1}{2}}\, W_{TOT}}{P_{M_S}} = \mu_r^{-\frac{1}{2}}\, Q_{M_S} \ \Rightarrow\ BW_{M_S}^{(\mu)} \sim \mu_r^{\frac{1}{2}}\, BW_{M_S} \end{aligned} \tag{23}$$

As regard the efficiency, firstly we define the losses in the materials. The following expression can be used for the dielectric losses:

$$L_d = \frac{\omega \varepsilon''}{2} \int\limits_{V_{sub}} |\mathbf{E}(r,\theta,\phi)|^2\ dV \tag{24}$$

and similarly for the magnetic losses:

$$L_m = \frac{\omega \mu''}{2} \int\limits_{V_{sub}} |\mathbf{H}(r,\theta,\phi)|^2\ dV \tag{25}$$

where $\varepsilon'' = \sigma_e/(\varepsilon_0\omega)$ and $\mu'' = \sigma_m/(\mu_0\omega)$. The total losses are therefore:

$$L_{TOT} = L_m + L_d \tag{26}$$

Considering an OM material with relations (4) and (14), it is immediate to write:

$$L_d^{(\mu)} = \mu_r^{-\frac{1}{2}}\ L_d\ ,\ L_m^{(\mu)} = \mu_r^{-\frac{3}{2}}\ L_m \tag{27}$$

where is supposed, for the sake of simplicity, the ES and OM to have the same loss-tangent; obviously this represents a "*fake*" ES with losses. In the losses definition (27) we use the mathematical substitution $V_{sub}^{(\mu)} = V_{sub}\, \mu_r^{-\frac{3}{2}}$; hence outside that volume there are no losses.

The radiation efficiency, defined as $\delta = P/(P + L_{TOT})$, can be now computed for ES and OM:

$$\delta_{J_S} = \frac{P_{J_S}}{P_{J_S} + L_d + L_m} \ , \ \delta_{M_S} = \frac{P_{M_S}}{P_{M_S} + L_d + L_m} \tag{28}$$

$$\delta^{(\mu)}_{J_S} = \frac{P_{J_S}}{P_{J_S} + \mu_r^{\frac{1}{2}} L_d + \mu_r^{-\frac{1}{2}} L_m} \ , \ \delta^{(\mu)}_{M_S} = \frac{P_{M_S}}{P_{M_S} + \mu_r^{-\frac{1}{2}} L_d + \mu_r^{-\frac{3}{2}} L_m} \tag{29}$$

The efficiencies in (28) and (29) are quite different compared to previous works, as [16]. Since this is a perturbation theory with a zero-order approximation model of the antenna (i.e. losses introduced by perturbation and no reference to a specific antenna geometry, but only to the stored energy) some differences were expected.
The obtained relations on the radiation properties (23), (28) and (29) allow to straightforwardly predict the advantage in using an OM material in presence of magnetic equivalent currents and the disadvantage with electric equivalent currents.
Starting from (19) dual relationships hold for antennas on OD (ε) materials:

$$BW^{(\varepsilon)}_{J_S} \sim \varepsilon^{1/2} \, BW_{J_S} \ , \ BW^{(\varepsilon)}_{M_S} \sim \frac{BW_{M_S}}{\varepsilon^{\frac{1}{2}}} \tag{30}$$

$$\delta^{(\varepsilon)}_{J_S} = \frac{P_{J_S}}{P_{J_S} + \varepsilon^{-\frac{3}{2}} L_d + \varepsilon^{-\frac{1}{2}} L_m} \ , \ \delta^{(\varepsilon)}_{M_S} = \frac{P_{M_S}}{P_{M_S} + \varepsilon^{-\frac{1}{2}} L_d + \varepsilon^{\frac{1}{2}} L_m} \tag{31}$$

C) Bandwidth and efficiency extension to a general domains relationship

Let us re-write the previous resonance energy-based theory with a general relationship between the E-fields in the form:

$$|\mathbf{E}(r, \theta, \phi)| = \mu_r^{-x} \ |\mathbf{E}_\mu(r_\mu, \theta, \phi)| \tag{32}$$

the solution for $\mathbf{H}_\mu$ would have the same relation as (32) but scaled by a factor of $\mu_r^{1/2}$:

$$|\mathbf{H}(r, \theta, \phi)| = \mu_r^{-x+\frac{1}{2}} \ |\mathbf{H}_\mu(r_\mu, \theta, \phi)| \tag{33}$$

Relations (32) and (33) directly affect the absolute value of the Poynting vector:

$$\begin{aligned} S^{(\mu)}_{J_S}(r, \theta, \phi) \ &= \mu_r^{2x-2} \ S_{J_S}(r, \theta, \phi) \\ S^{(\mu)}_{M_S}(r, \theta, \phi) \ &= \mu_r^{2x-1} \ S_{M_S}(r, \theta, \phi) \end{aligned} \tag{34}$$

By computing the bandwidth and efficiency, as in (23) and (29), the relations are exactly the same. This means that the relations on bandwidth (BW) and efficiency (δ) for an OM material compared to the ES, are invariant to an initial hypothesis on the OM material of the kind μ_r^{-x}. Dual relations developed for an OD show the same invariance. Therefore it is now possible to extend the theory to a wider set of antennas.
To give an example of its usefulness, we again consider two patch antennas, one with an OD material as substrate, the other in ES. The physical initial hypothesis of a constant radiated power (thus on $\mathbf{E}$) in the far-field without losses (differently from the dual case in (19)) will be:

$$|\mathbf{E}(r, \theta, \phi)| = \varepsilon_r^{-\frac{1}{2}} \, |\mathbf{E}_\varepsilon(r_\varepsilon, \theta, \phi)| \tag{35}$$

hence on **H**:

$$|\mathbf{H}(r,\theta,\phi)| = \varepsilon_r^{-1} \, |\mathbf{H}_\varepsilon(r_\varepsilon,\theta,\phi)| \tag{36}$$

Using the aforementioned invariance it is possible to say that the relations on bandwidth and efficiency will be again exactly the dual version of (30) and (31).

III NUMERICAL VALIDATION

The conclusions of the previous section are now validated by full-wave numerical simulation. For this purpose, CST Microwave Studio [11] is adopted.

A) Validation of fields inside a square patch

In order to validate the field relations, as a first example of application, we analyse a square patch, optimized to be resonant at 2.4 GHz by forcing the imaginary part of the impedance for both structures to be zero at the same frequency.
Two different patch configurations are compared:
i) the space between the patch and the ground plane consists of empty space (ES);
ii) the space between the patch and the ground plane consists of an OM material (with $\varepsilon_r = 1$, $\mu_r = 4$).
The resulting patch lengths were computed to be (Fig. 1): $L_a = 54$ mm and $L_b = 29.5$ mm. These dimensions approximately agree with the results obtainable from (5): it is noteworthy that the dimensions scaling is related to the effective permeability and not to the relative one.

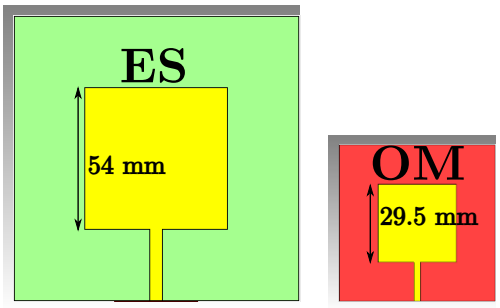

Figure 1: Top views of the analysed patch antennas: these antenna types are described mainly by magnetic current sources.

First of all, let us discuss the numerical results obtained with the two configurations in terms of the near-field regions of the two antennas. In Fig. 2 the simulated electric and magnetic near-fields of the two patch antennas are shown. The field values are taken on a cut plane in the middle of the substrate brick. These numerical results validate the relationships (4) and (14). The E-field of the patch, exploiting the OM-substrate, is approximately twice the one on the ES material, while the H-fields are approximately the same, considering for both fields evaluations a size compression by a factor of about two. Fig. 2 lets also to address the ambiguity when defining the volume V_{n-f} for the practical case. This can be done by interpreting V_{n-f} as the reactive region volume, thus "that portion of the near-field region immediately surrounding the antenna wherein the reactive

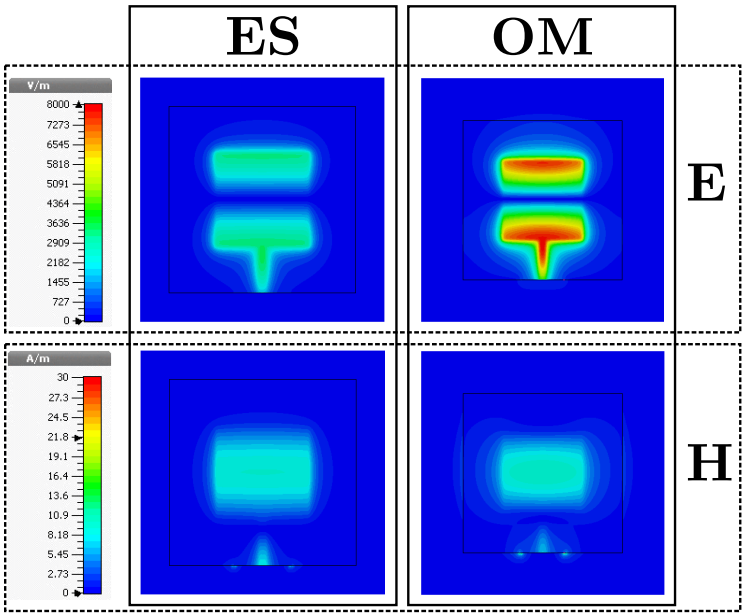

Figure 2: E and H near-field numerical simulation results of the two patches: the E-field for the antenna on the OM substrate is twice stronger and compressed in size than that on the ES.

field predominates". A common approximation for the boundary is a distance $d_{n-f} \simeq 0.62\sqrt{D^3/\lambda}$ from the antenna surface, where λ is the guided wavelength [12]. In Fig. 2, the fields are shown to be well confined inside that region, where d_{n-f} is approximately 40mm and 22mm for the ES and the OM material, respectively.
A difference of about 15% in terms of far-field radiated in the broadside direction is observed in Fig. 3. The reasons of this small discrepancy with respect to the previously developed theory can be ascribed to different spacings between the two radiating slots, which the patch antenna radiation mechanism is based on, in the OM and ES situations. From the far-field point of view the reduction of this distance in the OM case is a direct consequence of the corresponding directivity reduction, since the two slots-array has a shorter step. This is also confirmed by the further widening of the radiation surface of a more miniaturized square patch exploiting a denser OM material, as confirmed by simulation.

B) Validation of bandwidth relations

As a further test we compare different antenna layouts from the operating bandwidth point of view: the same miniaturized patch antenna (thus exploiting magnetic equivalent surface currents) and a single full-wavelength loop antenna (exploiting electric equivalent surface currents) embedded in the substrate. In these cases two substrates are considered: the same OM as before and the dual only-dielectric (OD) substrate ($\varepsilon_r = 4$, $\mu_r = 1$), in order to validate the previous theoretical results. The patch antenna keeps the same size for both substrates, since the field is well confined between the conductors, hence the effective parameters have a negligible variation. The loop antennas, whose layouts are shown in Fig. 4, have slightly different sizes, since the fringing of the field in these open structures significantly depends on the electromagnetic characteristics of the substrates: the loop line

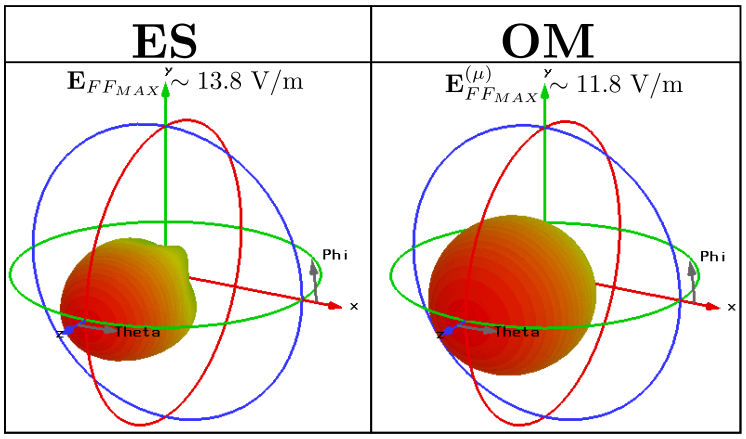

Figure 3: E far-field numerical simulation results of the two patches: the $E^{(\mu)}_{FF}$-field maximum value for the antenna on the OM substrate is different than that on the empty space.

width is 1 mm, while the inner radius length provides a full-wavelength behaviour at 2.4 GHz.

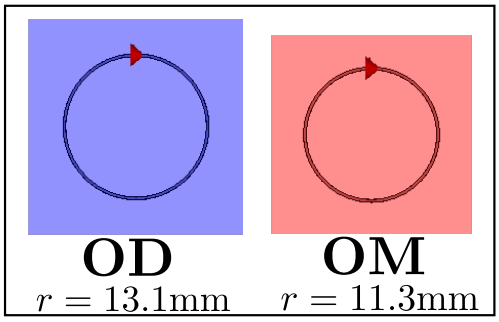

Figure 4: Top views of the analysed loop antennas: these antenna types are described mainly by electric current sources.

In Fig. 5 the reflection coefficients for the patch on OM and OD are shown. It is clear the advantage in terms of bandwidth by using the OM with respect to the OD: it is increased approximately by a factor of 4, as predicted by our theory.
Once again in Fig. 6 the reflection coefficients are shown, this time for two loop antennas on the same OD and OM as before. In this case it is clear the advantage in using the OD instead of the OM: the bandwidths are again approximately related by a factor of 4.

C) Simulations with realistic losses and dispersion

Today's available magneto-dielectric materials have relevant losses and are subject to permeability dispersion.
As an example regarding the losses, in [5] the loss tangent is about 0.38 at 900MHz and it is significantly higher than available OD materials. This obviously results in lower efficiency when using a real MD; in particular the relations (28) and (29) will have heavily different L_m and L_d inside. It is thus still disadvantageous to use present MD materials if the application interest is purely on the efficiency. On the other hand, in this case the

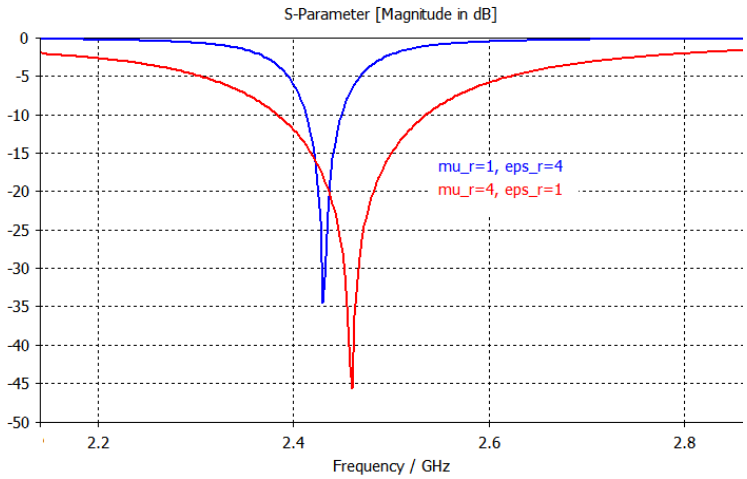

Figure 5: S_{11} for the patch antennas. It is normalized to the antennas impedance at resonance (250 and 325 ohm for the OM and OD patches, respectively).

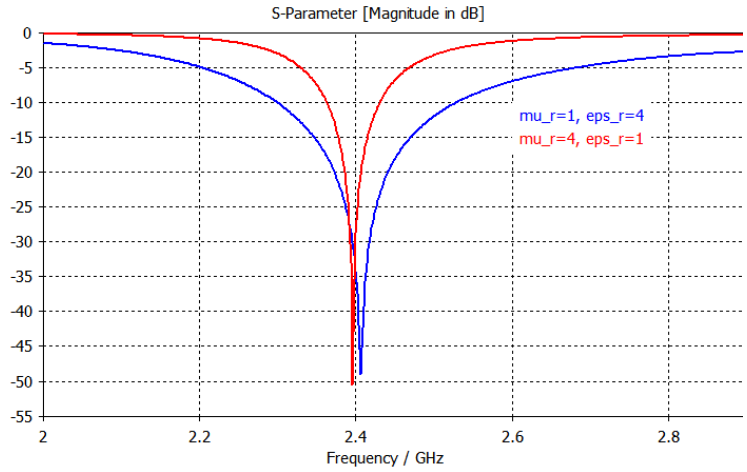

Figure 6: S_{11} for the loop antennas. It is normalized to the antennas impedance at resonance (60 vs 66 ohm for the OM and OD loop, respectively).

bandwidth is obviously further increased due to the increased losses when compared to the energy stored.
An extensive work on frequency dispersion is provided in [17]. Most materials containing magnetic inclusions are subject to the Ferro-Magnetic Resonance, which brings a strong dispersion in its vicinity. As a result, there could be a huge difference in terms of radiation properties.

IV CONCLUSION

We have provided an analytical method for demonstrating the relationship between the antenna topologies and high permeability and/or high permittivity substrates, for

miniaturization purposes. We have proposed a novel definition for the region pertaining to the antenna near-field and for the associated field strength. On the surface of this region we have computed the equivalent magnetic and electric current sources and we have shown that the radiation performances and the operating frequency bandwidth of an antenna, which is mainly based on magnetic sources, are improved by the introduction of high permeability materials. Dually, high permittivity materials allow to improve the same performances in case of an antenna which is mainly based on electric sources.
The results have been validated by full-wave numerical simulations of some reference topologies. These are consistent with previous dedicated approaches, based on approximated models suitable for selected topologies, and confirm, by an independent theoretical and general way, the surface current relation conjectured in [7].
Being based on a resonance condition, the method is limited to this class of antennas. Other limitations are due to the simplifications introduced to the medium, as isotropy, non-dispersion and loss-free. These can be partly addressed using a perturbation theory. The rule of thumb in designing the antenna, is to first choose a topology on the ES and find its main sources in order to immediately choose the loading material. It is then possible to proceed on a normal process of design and optimization, but performed on the selected magneto-dielectric medium, whose size should be enough to keep inside the major part of the reactive near-field.

ACKNOWLEDGEMENTS

This work was partly funded by the Italian Ministry of Defence, within the framework of the national project "Antenna Engineered piezo-magnetic composites for wearable miniaturized antennas" and by the COST Action IC1301 - Wireless Power Transmission for Sustainable Electronics (WIPE).

REFERENCES

[1] A. Costanzo, F. Donzelli, D. Masotti, and V. Rizzoli: "Rigorous design of RF multi-resonator power harvesters", *Proc. of the 4th EuCAP*, pp. 1-4, 2010.

[2] J. S. Ho, S. Kim, and A. S. Y. Poon: "Midfield wireless powering for implantable systems", *Proc. IEEE*, 101, 1369 (2013).

[3] H. Mosallaei, K.Sarabandi: "Magneto-dielectrics in electromagnetics: concept and applications", *IEEE Transactions on Antennas and Propagation*, vol.52, no.6, pp. 1558- 1567, June 2004.

[4] H. Mosallaei, K. Sarabandi: "Engineered meta-substrates for antenna miniaturization", *URSI International Symposium on Electromagnetic Theory*, Pisa, Italy, May 23-27, 2004.

[5] M. Aldrigo, A. Costanzo, D. Masotti, C. Baldisserri, I. Dumitru, and C. Galassi: "Numerical and experimental characterization of a button-shaped miniaturized UHF antenna on magneto-dielectric substrate", *International Journal of Microwave and Wireless Technologies*, vol. 5, no. 3, pp. 231–239, 2013.

[6] M. Aldrigo, A. Costanzo, D. Masotti, C. Galassi: "Exploitation of a novel magneto-dielectric substrate for miniaturization of wearable UHF antennas", *Elsevier Material Letters*, Vol. 87, pp. 127-130, Aug. 2012.

[7] Karilainen, A.O.; Ikonen, P.M.T.; Simovski, C.R.; Tretyakov, S.A.: "Choosing Dielectric or Magnetic Material to Optimize the Bandwidth of Miniaturized Resonant Antennas", *Antennas and Propagation, IEEE Transactions on* , vol.59, no.11, pp.3991,3998, Nov. 2011.

[8] P. Ikonen and S. Tretyakov: "On the advantages of magnetic materials in microstrip antenna miniaturization", *Microwave and Optical Technology Letters*, vol. 50, no. 12, pp. 3131–3134, 2008.

[9] Mikki, S.M.; Antar, Y.M.M.: "A Theory of Antenna Electromagnetic Near Field - Part I", *Antennas and Propagation, IEEE Transactions on* , vol.59, no.12, pp.4691,4705, Dec. 2011

[10] A. E. H. Love: "The integration of equations of propagation of electric waves", *Trans. Roy. Soc. London*, pp. 1-45, 1901.

[11] ©2014 CST Computer Simulation Technology AG. All rights reserved.
Website: `http://www.cst.com`

[12] C. A. Balanis: "Antenna Theory: Analysis and Design, 3rd Edition". Wiley-Interscience, 2005, p. 34.

[13] V. Rizzoli and A. Lipparini: "Propagazione Elettromagnetica Guidata", vol. 1. Progetto Leonardo, 1991.

[14] Pacini, A.; Costanzo, A.; Masotti, D.: "A theoretical and numerical approach for selecting miniaturized antenna topologies on magneto-dielectric substrate's", *European Microwave Conference (EuMC), 2014 44th*, pp.869,872, 6-9 Oct. 2014

[15] C. H. Wilcox: "An expansion theorem for electromagnetic fields", *Communications on Pure and Applied Mathematics*, vol.9, no.2, pp.115–134, May 1956

[16] R. C. Hansen, M. Burke: "Antennas with magneto-dielectrics", *Microwave and optical technology letters*, vol.26, no. 2, pp.75-78, Jun. 2000

[17] P. M. T. Ikonen, K. N. Rozanov, A. V. Osipov, P. Alitalo, and S. A. Tretyakov: "Magnetodielectric substrates in antenna miniaturization: Potential and limitations", *IEEE Transactions on Antennas and Propagation*, vol. 54, pp. 3391–3399, Mar. 2006.

Biographies

Alex Pacini received the bachelor's degree with honours in electrical, computer science, and telecommunication engineering at the Second Faculty of Engineering of the University of Bologna, Italy, in October 2012. His dissertation titled "Study of antenna topologies over MD substrates" was dedicated to the theoretical study of antennas on MDs and to defining design rules for antenna topologies, resulting in the best compromise between miniaturization and radiation efficiency. He is currently toward the end of his master's degree in electrical and telecommunication

engineering for the sustainable development at the same university. In Fall 2013 he was awarded with the MTT-S Undergraduate/Pregraduate Scholarship Awards. He is a student member of MTT-S and IEEE Antennas and Propagation Society.

Alessandra Costanzo (M'99–SM'13) is Associate Professor of electromagnetic fields at the University of Bologna, Italy. She has authored more than 140 scientific publications on peer reviewed international journals and conferences, three chapter books; she holds three international patents. She has developed innovative software platform for the nonlinear/electromagnetic co-simulation of RF systems, excited by modulated sources demonstrating circuit-level analysis of entire MIMO and UWB links, including realistic channel models. She is now involved in wearable energy-autonomous sensors and wireless power transfer systems. She is MC member of the EU COST action WiPE "Wireless power transfer for sustainable electronics" and she chairs WG1: "far-field wireless power transfer". She is TPC member of MTT-S IMS, EUMW, WPTC, RFID-TA ICUWB. She is vice chair of IEEE MTT-S TC-26 "Wireless Energy Transfer and Conversion" and member of IEEE MTT-S TC-24 RFID Technologies.

Diego Masotti (M'00) received the Dr. Ing. degree in electronic engineering and Ph.D. degree in electric engineering from the University of Bologna, Bologna, Italy, in 1990 and 1997, respectively. In 1998 he joined the University of Bologna as a Research Associate of electromagnetic fields. He has co-authored more than 120 scientific publications on peer reviewed International Journals and conferences. His research interests are in the areas of nonlinear microwave circuit simulation and design, and nonlinear/electromagnetic co-design of integrated subsystems/systems. Dr. Masotti has been a member of the Paper Review Board of the IEEE TRANSACTIONS ON MICROWAVE THEORY AND TECHNIQUES, IEEE Communication Letters, IET-Circuit Devices & Systems, IEEE MICROWAVE AND WIRELESS COMPONENTS LETTERS, since 2004, 2010, 2011, and 2013, respectively. He is also member of the Technical Program Committee (TPC) board of the IEEE Microwave Theory and Techniques Society (IEEE MTT-S) European Microwave Week (EUMW).

List of figures and tables

Fig. 1. Top views of the analysed patch antennas: these antenna types are described mainly by magnetic current sources.

Fig. 2. E and H near-field numerical simulation results of the two patches: the E-field for the antenna on the OM substrate is twice stronger and compressed in size than that on the ES..

Fig. 3. E far-field numerical simulation results of the two patches: the $E_{FF}^{(\mu)}$-field maximum value for the antenna on the OM substrate is different than that on the empty space.
Fig. 4. Top views of the analysed loop antennas: these antenna types are described mainly by electric current sources.
Fig. 5. S_{11} for the patch antennas. It is normalized to the antennas impedance at resonance (250 and 325 ohm for the OM and OD patches, respectively).
Fig. 6. S_{11} for the loop antennas. It is normalized to the antennas impedance at resonance (60 vs 66 ohm for the OM and OD loop, respectively).